Available online at http://ijim.srbiau.ac.ir/
Int. J. Industrial Mathematics (ISSN 2008-5621)
Vol. 7, No. 3, 2015 Article ID IJIM-00628, 14 pages
Research Article

MHD boundary layer heat and mass transfer of a chemically reacting Casson fluid over a permeable stretching surface with non-uniform heat source/sink

B. J. Gireesha *†, B. Mahanthesh ‡§, M. M. Rashidi ¶

Abstract

The heat and mass transfer analysis for MHD Casson fluid boundary layer flow over a permeable stretching sheet through a porous medium is carried out. The effect of non-uniform heat generation/absorption and chemical reaction are considered in heat and mass transport equations correspondingly. The heat transfer analysis has been carried out for two different heating processes namely; the prescribed surface temperature (PST) and prescribed surface heat flux (PHF). After transforming the governing equations into a set of non-linear ordinary differential equations, the numerical solutions are generated by an efficient Runge-Kutta-Fehlberg fourth-fifth order method. The solutions are found to be dependent on physical parameters such as Casson fluid parameter, magnetic parameter, porous parameter, Prandtl and Schmidt number, heat source/sink parameter, suction/injection parameter and chemical reaction parameter. Typical results for the velocity, temperature and concentration profiles as well as the skin-friction coefficient, local Nusselt number and local Sherwood number are presented for different values of these pertinent parameters to reveal the tendency of the solutions. The obtained results are compared with earlier results with some limiting cases of the problem and found to be in good agreement.

Keywords : Casson fluid; Heat mass transfer; Non-uniform heat source/sink; Numerical solution; Porous medium; Chemical reaction; Stretching sheet.

1 Introduction

The problems of heat, mass and momentum transfer in the boundary layer towards stretching surface have received great attention during the last decades owing to the abundance of practical applications. Particularly, in chemical and manufacturing processes such as polymer extrusion, enhanced oil recovery, metal spinning, packed bed catalytic reactors, transpiration cooling, continuous casting of metals, glass and fiber production, hot rolling of paper and wire drawing. Sakiadis [1] did a pioneering work on boundary layer flow on a continuously moving stretch-

*Corresponding author. bjgireesu@rediffmail.com
†Department of Mechanical Engineering, Cleveland State University, Cleveland, OHIO, USA.
‡Department of Mechanical Engineering, Cleveland State University, Cleveland, OHIO, USA.
§Department of Studies and Research in Mathematics, Kuvempu University, Shankaraghatta-577 451, Shimoga, Karnataka, India.
¶DShanghai Key Lab of Vehicle Aerodynamics and Vehicle Thermal Management Systems, Tongji University, Address: 4800 Cao An Rd., Jiading, Shanghai 201804, China.

ing surface. Thereafter, numerous investigations were made on the heat and mass transfer over a stretching surface in different directions ([2]-[5]). On the other hand, the influence of magnetic field is important in MHD generators, bearings, pumps and several industrial equipments. Its relevance can also be seen in the boundary layer control which is affected by the interaction between the magnetic field and an electrically conducting fluid. Keeping this in view, many investigators have shown their interest to study the behavior of boundary layers in the presence of a transverse magnetic field (see [6]-[10]).

All the above-said investigations are regarding "heat and mass transfer analysis of Newtonian fluid". Some fluids like blood, food stuffs, slurries, molten plastics, polymeric liquids, artificial fibers and synovial fluid exhibit non-Newtonian fluid characteristics. Such fluids exhibit shear-stress-strain relationships which diverge significantly from the Newtonian model. Most of non-Newtonian models involve some form of modification to the momentum conservation equations [11]. In the category of non-Newtonian fluids, the Casson fluid has distinct features and was presented by Casson in 1995 [12]. It has significant applications in polymer processing industries and biomechanics. The Casson fluid model is sometimes stated to fit rheological data better than the general viscoplastic model for many materials [13].

Elbade and Salwa [14] investigated the heat transfer characteristics of Casson fluid flow between rotating cylinders in the presence of a magnetic field. Boyd et al [15] analyzed the Casson and Carreau-Yasuda non-Newtonian blood models with steady and oscillatory flow. They employed Lattice Boltzmann method to solve the governing equations. Hayat et al [16] obtained the series solutions for MHD Casson fluid flow over a stretched surface with Soret and Dufour effects. Mustafa et al [17] discussed an unsteady boundary layer flow of Casson fluid due to an impulsively started moving flat plate. Later, the magnetohydrodynamic boundary layer flow of a Casson fluid over an exponentially shrinking permeable sheet has been analyzed by Nadeem et al [18]. Recently, Swati et al [19] have studied two dimensional boundary layer flow and heat transfer of Casson fluid over an unsteady stretching surface.

On the other hand, the study of flow and heat transfer in porous media has received much attention due to its industrial and technological applications. Other porous media problems like insulation engineering and geo-mechanics, Darcy porous media model have been employed in convectional approach to simulate pressure drop across the porous regime. It is important to note that, porous materials can be used to enhance the rate of heat transfer from stretching surfaces. An excellent literature review on flow through porous media can be found viz. Starov and Zhdanov [20], Kiwan and Ali [21], Rashidi and Esmaeel [22], Tamayol et al [23], Gireesha et al [24], Sheikholeslami and Ganji [25], Rashidi et al [26]. Further, in many engineering applications, the effect of wall mass transfer has their own importance, for instance, in thermal oil recovery, thrust bearing and radial diffusers. Its relevance is also seen in adding and removing reactants in chemical processes. In view of these applications, the effect of uniform suction on nanofluid flow and heat transfer due to a stretching cylinder was examined by Sheikholeslami [27]. He found that, the wall shear stress is increased by strengthening suction effect. Pramanik [29] examined the Casson fluid flow and heat transfer towards an exponential porous stretching surface in the presence of suction/blowing. Recently, Tufail et al [28] have studied the suction/blowing effect on Casson fluid flow and heat transfer over porous stretching surface with heat source/sink.

Heat source/sink effects are crucial in controlling the heat transfer. Many studies considered merely the uniform heat source/sink effect, i.e., temperature dependent heat source/sink (see [29]-[32]). But different from these, Eldahab and El-Aziz [33] have included the effect of non-uniform heat source/sink with suction/blowing. Abel et al [34] and Dulal [35] have also studied the effect of non-uniform heat source/sink on heat transfer analysis. Recently, Gireesha et al [36] studied the boundary layer flow and heat transfer of dusty fluid over a stretching sheet with non-uniform heat source/sink.

The focal impartial of the current study is to deliberate the similarity solution to the problem of two-dimensional boundary layer flow, heat and mass transfer of non-Newtonian Casson fluid over a porous stretching surface. To incorporate the porous medium effect, the well known

Darcy model has been used. In addition, the effects of space and temperature dependent heat source/sink and homogeneous chemical reaction are included. Using suitable similarity transformations, the governing partial differential equations are converted into a set of non-linear ordinary differential equations, and then they are solved numerically.

2 Nomenclature

a Stretching rate
b, c, D Constants
A^*, B^* Space and temperature dependent heat generation/absorption
B_0 Magnetic field strength
C Concentration of the fluid
C_f Skin friction co-efficient
c_p Specific heat
C_w Concentration at the wall
C_∞ Ambient fluid concentration
D_m Mass diffusivity
e_ij Strain tensor rate
k Thermal conductivity
k^* Permeability of the porous medium
k_0 Porous parameter
Kc Chemical reaction parameter
M^2 Magnetic parameter
m_w Mass flux
Nu_x Local Nusselt number
Pr Prandtl number
p_y Yield stress of the fluid
q_w Surface heat flux
q''' Space and temperature dependent heat generation/absorption
R Chemical reaction rate
S Suction/blowing parameter
Sc Schmidt number
Sh Sherwood number
T Temperature of the fluid
T_w Temperature at the wall
T_∞ Ambient fluid temperature
u, v Velocity components along x and y directions
U_w Stretching velocity
V_w Suction/Blowing velocity
x Coordinate along the stretching sheet
y Distance normal to the stretching sheet

Greek symbols

ν Kinematic viscosity
φ Dimensionless concentration
π Product of component of deformation rate with itself
π_c Critical value of product of the component of the rate of strain tensor with itself
μ_B Plastic dynamic viscosity of the non-Newtonian fluid
ρ Density of the fluid
σ Electric conductivity of the fluid
θ Dimensionless temperature
ψ Stream function
η Similarity variable
τ_w Surface shear stress
γ Casson fluid parameter.

3 Description of the Problem

Consider a steady two-dimensional laminar flow an incompressible electrically conducting Casson fluid over a stretching surface through a porous medium. The sheet coincides with the plane $y = 0$ and the flow is confined to $y > 0$. The flow is generated due to linear stretching of the sheet caused by simultaneous application of two equal and opposite forces along the x-axis. The flow field is exposed due to the influence of a uniform transverse magnetic field of strength B_0 as shown in the figure 1. Keeping the origin

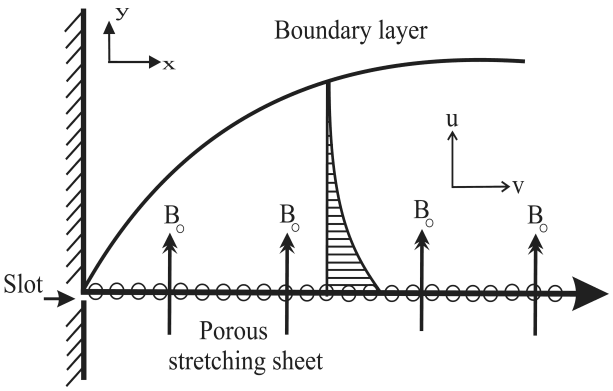

Figure 1: Flow configuration and coordinate system of the problem.

fixed, the sheet is then stretched with a velocity $U_w(x) = ax$, where $a > 0$ is the stretching rate. It is assumed that the magnetic Reynolds number is very small, so that an induced magnetic field is neglected. The rheological equation of state for an isotropic and incompressible Casson fluid can

Table 1: Comparison results for skin friction co-efficient $(1+\frac{1}{\gamma})f''(0)$ in the case $k_0 = 0, S = 0$ and $M = 0.5$.

γ	0.8	1.4	2.0	3.0
Hayat et al [16]	1.67705	1.46385	1.36931	1.29099
Present study	1.67712	1.46386	1.36931	1.29099

Table 2: Comparison results for skin friction co-efficient $f''(0)$ in the case $\gamma = \infty, k_0 = 0$ and $S = 0$.

M^2	0.0	0.5	1.0	1.5	2.0	2.5	3.0
Cortel [4]	1.00000	1.22475	1.41421	1.58114	1.73205	-	-
Tufail et al [28]	1.00000	1.22474	1.41421	1.58114	1.73205	1.87083	2.00000
Present study	1.00004	1.22477	1.41421	1.58113	1.73205	1.87082	2.00000

Table 3: Numerical results of $C_f = (1 + 1/\gamma)f''(0)$, $-\theta_\eta(0)$ and $-\varphi_\eta(0)$ for different values of $M^2, k_0, \gamma, A^*, B^*, Pr$ and Sc.

M^2	k_0	γ	A^*	B^*	Pr	Sc	$f''(0)$ $S=+0.5$	$f''(0)$ $S=-0.5$	$-\theta_\eta(0)$ $S=-0.5$	$-\varphi_\eta(0)$ $S=-0.5$
0.5	2.0	1.0	0.05	0.05	0.72	0.22	-2.7122	-2.21223	0.91466	0.42235
1.0							-3.08946	-2.58946	0.87918	0.4056
2.0							-3.42214	-2.92214	0.84985	0.39285
2.0	0.0	1.0	0.05	0.05	0.72	0.22	-2.71222	-2.21223	0.91466	0.42235
	1.5						-3.2604	-2.7604	0.86387	0.39883
	2.5						-3.57603	-3.07603	0.83693	0.3875
2.0	2.0	0.3	0.05	0.05	0.72	0.22	-4.91151	-4.41151	0.95919	0.44596
		0.8					-3.61341	-3.11341	0.86816	0.4007
		1.5					-3.14756	-2.64756	0.82068	0.38095
2.0	2.0	1.0	0.1	0.05	0.72	0.22	-3.42214	-2.92214	0.8244	0.39285
			0.3				-3.42214	-2.92214	0.72258	0.39285
			0.5				-3.4221	-2.92214	0.62077	0.39285
2.0	2.0	1.0	0.05	0.05	0.72	0.22	-3.42214	-2.92214	0.84985	0.39285
				0.1			-3.42214	-2.92214	0.79455	0.39285
				0.15			-3.42214	-2.92214	0.73009	0.39285
2.0	2.0	1.0	0.05	0.05	0.72	0.22	-3.42214	-2.92214	0.84985	0.39285
					7.0		-3.42214	-2.92214	5.35527	0.39285
					10		-3.42214	-2.92214	7.11842	0.39285
2.0	2.0	1.0	0.05	0.05	0.72	0.22	-3.42214	-2.92214	0.84985	0.39285
						0.60	-3.42214	-2.92214	0.84985	0.79971
						0.96	-3.42214	-2.92214	0.84985	1.16011

be written as [16]:

$$\tau_{ij} = \left(\mu_B + \frac{p_y}{\sqrt{2\pi}}\right) 2e_{ij} \qquad \pi > \pi_c,$$
$$\tau_{ij} = \left(\mu_B + \frac{p_y}{\sqrt{2\pi_c}}\right) 2e_{ij} \qquad \pi < \pi_c, \tag{3.1}$$

where

$$e_{ij} = \frac{1}{2}\left(\frac{\partial u_i}{\partial x_j} + \frac{\partial u_j}{\partial x_i}\right) \tag{3.2}$$

is the rate of strain tensor, μ_B -plastic dynamic viscosity of the non-Newtonian fluid, p_y -yield stress of the fluid, π -product of component of deformation rate with itself, π_c -critical value of product of the component of the rate of strain tensor with itself and u_i's are velocity components.

Under usual boundary layer approximations; the conservation of mass, momentum, energy and concentration equations for Casson fluid are re-

spectively given as [16];

$$\frac{\partial u}{\partial x}+\frac{\partial v}{\partial y} = 0, \tag{3.3}$$

$$u\frac{\partial u}{\partial x}+v\frac{\partial v}{\partial y} = \nu\left(1+\frac{1}{\gamma}\right)\frac{\partial^2 u}{\partial y^2} - \frac{\sigma {B_0}^2}{\rho}u-\frac{\nu}{k^*}u, \tag{3.4}$$

$$u\frac{\partial T}{\partial x}+v\frac{\partial T}{\partial y} = \frac{k}{\rho c_p}\frac{\partial^2 T}{\partial y^2}+\frac{1}{\rho c_p}q''', \tag{3.5}$$

$$u\frac{\partial C}{\partial x}+v\frac{\partial C}{\partial y} = D_m\frac{\partial^2 C}{\partial y^2}-R(C-C_\infty), \tag{3.6}$$

where u and v are velocity components along x and y directions respectively, ν is kinematic viscosity of the fluid, $\gamma = \frac{\mu_B\sqrt{2\pi_c}}{p_y}$ is the Casson fluid parameter, σ is electrical conductivity of the fluid, B_0 is uniform magnetic field, k^* is permeability of the porous medium, ρ is fluid density, T is the temperature of the fluid, k is thermal conductivity of the fluid, c_p is the specific heat at constant pressure, C is concentration of the fluid, D_m is mass diffusivity and q''' is the space and temperature dependent heat generation/absorption, which can be expressed as [34];

$$q''' = \frac{kU_w(x)}{x\nu}\left(A^*(T_w-T_\infty)f'(\eta) + B^*(T-T_\infty)\right), \tag{3.7}$$

where A^* and B^* are parameters of space and temperature dependent heat generation or absorption. It is to be noted that $A^* > 0$ and $B^* > 0$ correspond to internal heat generation, whereas $A^* < 0$ and $B^* < 0$ correspond to internal heat absorption. The thermal boundary conditions depend on the type of heating process under consideration. In this study heat transfer analysis has been carried out for two different heating processes namely prescribed surface temperature and prescribed heat flux. Boundary conditions for the flow and mass transfer are considered as follows;

$$\begin{aligned} &u = U_w(x),\ v = V_w(x),\\ &C = C_w = C_\infty + cx,\\ &T = T_w = T_\infty + bx,\ \text{(PST case)}\\ -k\frac{\partial T}{\partial y} &= q_w(x) = Dx\ \text{(PHF case) at}\quad y = 0,\\ &u\to 0,\ T\to T_\infty,\ C\to C_\infty\ \text{ as }\ y\to\infty, \end{aligned} \tag{3.8}$$

where $U_w(x) = ax$ is the stretched velocity, c is a positive constant and $V_w(x)$ is suction/blowing velocity at the wall. It should be noted that $V_w(x) > 0$ corresponds velocity of suction and $V_w(x) < 0$ corresponds velocity of blowing. Let us introduce the dimensionless variables f, φ and the similarity variable η as

$$\begin{aligned} \psi(x,y) &= (U_w x\nu)^{\frac{1}{2}}f(\eta),\\ T &= T_\infty + (T_w-T_\infty)\varphi(\eta),\\ C &= C_\infty + (C_w-C_\infty)\varphi(\eta),\\ \eta &= \left(\frac{U_w}{\nu x}\right)^{\frac{1}{2}}y, \end{aligned} \tag{3.9}$$

here, $T = bx\theta(\eta)+T_\infty$ (PST case), $T-T_\infty = \frac{Dx}{k}\sqrt{\frac{\nu}{a}}\theta(\eta)$ (PHF case), T_w and T_∞ are denotes the temperature at the wall and at large distance from the wall respectively, C_w and C_∞ denote the concentration at the wall and at large distance from the wall respectively and $\psi(x,y)$ is the physical stream function which automatically ensures mass conservation equation (3.3), velocity components are readily obtained as

$$\begin{aligned} u &= \partial\psi/\partial y = ax\,f'(\eta),\\ v &= -\partial\psi/\partial x = -\sqrt{\nu a}\,f(\eta), \end{aligned} \tag{3.10}$$

On substituting equations (3.9) and (3.10) into equations (3.4)-(3.6), we obtain following set of ordinary differential equations.

$$\left(1+\frac{1}{\gamma}\right)f'''(\eta)+f(\eta)f''(\eta)-f'(\eta)^2 -(M^2+k_0)f'(\eta) = 0, \tag{3.11}$$

$$\theta''(\eta)+Pr\left(f(\eta)\theta'(\eta)-f'(\eta)\theta(\eta)\right) +A^*f'(\eta)+B^*\theta(\eta) = 0, \tag{3.12}$$

$$\varphi''(\eta)+Sc\left(f(\eta)\varphi'(\eta) -f'(\eta)\varphi(\eta)\right) = 0. \tag{3.13}$$

Boundary conditions given in (3.8) will take the following form;

$$\begin{aligned} &f'(\eta) = 1,\ f(\eta) = S,\ \varphi(\eta) = 1,\\ &\theta(\eta) = 1,\ \text{(PST case)},\\ &\theta'(\eta) = -1,\ \text{(PHF case)}\ \text{ at }\ \eta = 0,\\ &f'(\eta)\to 0,\ \theta(\eta)\to 0,\\ &\varphi(\eta)\to 0\ \text{ as }\ \eta\to\infty, \end{aligned} \tag{3.14}$$

where $M^2 = \frac{\sigma {B_0}^2}{\rho a}$ -magnetic parameter, $k_0 = \frac{\nu}{k^* a}$ -permeability parameter, $S = \frac{V_w(x)}{\sqrt{\nu a}}$ -suction/blowing parameter, $Pr = \frac{\mu c_p}{k}$ -Prandtl

number, $Sc = \frac{\nu}{D_m}$ -Schmidt number and $Kc = \frac{R}{a}$ -chemical reaction parameter.

If $\gamma \to \infty$, $M^2 = k_0 = 0$, then the equation (3.11) subjected to boundary conditions (3.14) admits the closed-form analytical solution, which was reported by [3];

$$f(\eta) = (1 - e^{\eta}). \tag{3.15}$$

Physical quantities of interest are the skin friction coefficient (C_f) and local Sherwood number (Sh), which are defined as

$$\begin{aligned} C_f &= \frac{\tau_w}{\rho {U_w}^2}, \; Nu = \frac{q_w}{k(T_w - T_\infty)}, \\ Sh &= \frac{m_w}{D_m(C_w - C_\infty)}, \end{aligned} \tag{3.16}$$

where τ_w is the surface shear stress, q_w is the surface heat flux and m_w is the mass flux, which are given by

$$\begin{aligned} \tau_w &= \mu \left(\frac{\partial u}{\partial y}\right)_{y=0}, \\ q_w &= -k \left(\frac{\partial T}{\partial y}\right)_{y=0}, \\ m_w &= -D_m \left(\frac{\partial C}{\partial y}\right)_{y=0}. \end{aligned} \tag{3.17}$$

In view of similarity variables, the equation (3.16) we obtain

$$\begin{aligned} \sqrt{Re_x} C_f &= \left(1 + \frac{1}{\gamma}\right) f''(0), \\ {Re_x}^{-\frac{1}{2}} Nu &= -\theta'(0) \\ Sh(Re_x)^{-1/2} &= -\varphi'(0), \end{aligned} \tag{3.18}$$

where $Re_x = \frac{U_w x}{\nu}$ is the local Reynolds number.

4 Numerical Method and Validation

The equations (3.11)-(3.13) are highly non-linear in nature, hence the exact solution do not seem to be feasible. Therefore, these equations with subject to boundary conditions (3.14) are solved numerically by Fehlberg fourth-fifth order Runge-Kutta method using Maple. In this package, two sub methods are available, namely trapezoidal and midpoint method. To solve this kind of two point boundary value problem the trapezoidal

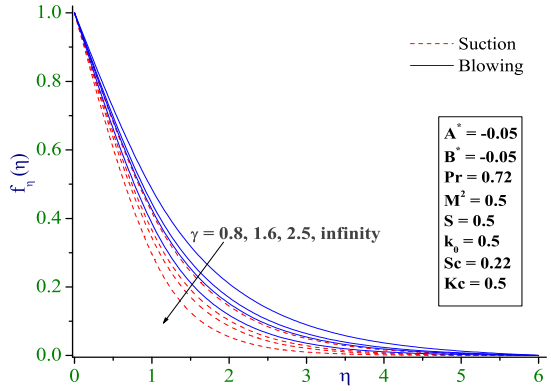

Figure 2: Effect of γ on velocity profile.

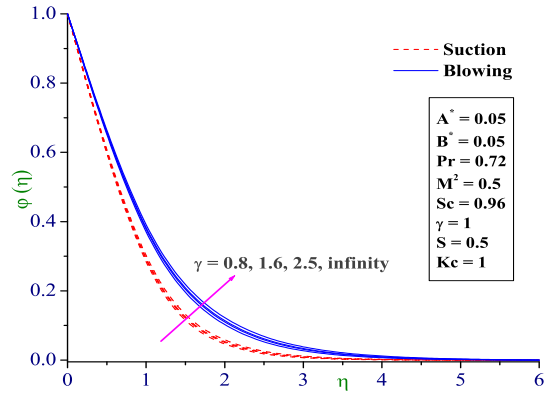

Figure 3: Effect of γ on concentration profile.

method is generally efficient, but it is incapable to handle harmless endpoint singularities, but this can able in midpoint method. Thus, the midpoint method with the Richardson extrapolation enhancement scheme is chosen as a sub method. The asymptotic boundary conditions at η_∞ were replaced by those at η_∞ in accordance with standard practice in the boundary layer analysis. Additionally, the relative error tolerance for convergence is considered to be 10^6 throughout our numerical computation.

To assess the accuracy of aforementioned numerical method, comparison of skin friction coefficient $\left(1 + \frac{1}{\gamma}\right) f''(0)$ values between the present results and existing results for various values of Casson fluid parameter (γ) with $k_0 = S = 0$ is presented in the Table 1. In addition, comparison of present results of $f''(0)$ values with those of Cortel [4] and Tufail et al [28] for the case $\gamma \to \infty, k_0 = 0$ and $S = 0$ is also made and

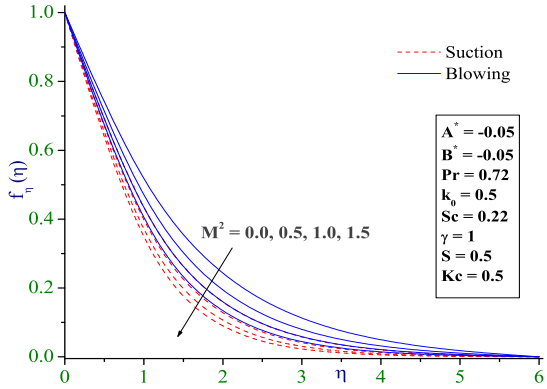

Figure 4: Effect of M^2 on velocity profile.

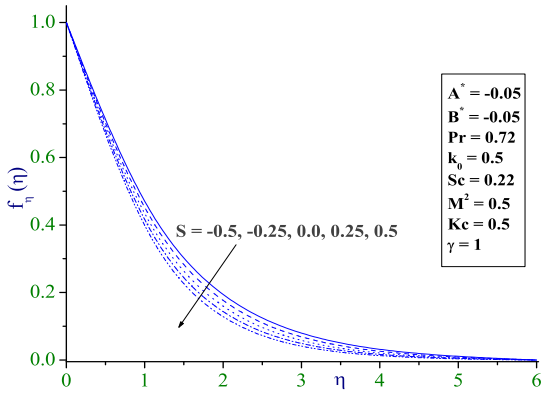

Figure 6: Effect of S on velocity profile.

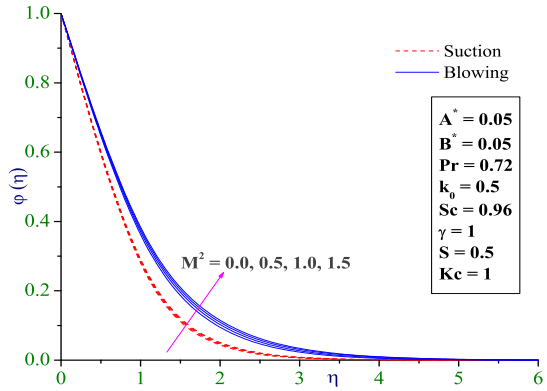

Figure 5: Effect of M^2 on concentration profile.

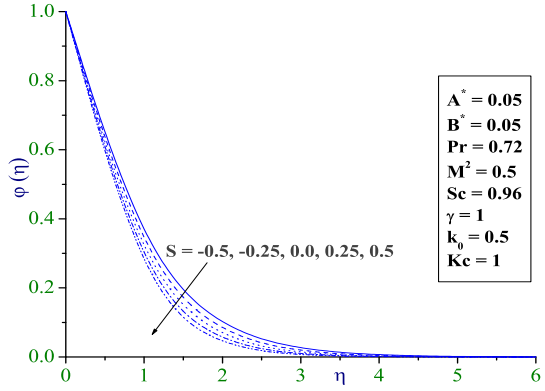

Figure 7: Effect of S on concentration profile.

presented in Table 2. Tables 1 and 2 are showed a very good agreement with these approaches and thus verifies the accuracy of the method used.

5 Results and Discussion

The main aim of this section is to analyze the effects of various physical parameters like Casson fluid parameter (γ), suction/injection parameter (S), magnetic parameter (M^2), porous parameter (k_0), Prandtl number (Pr), space-dependent heat source/sink parameter (A^*), temperature-dependent heat source/sink parameter (B^*), chemical reaction parameter (Kc) and Schmidt number (Sc) on different flow fields. The figures 2-18 have been plotted for such objective. It is worth mentioning that the present study reduces to the classical Newtonian fluid study, when $\gamma \to \infty$. The impact of some physical parameters of the present problem on skin friction coefficient $(1 + 1/\gamma)f''(0)$, local Nusselt number $-\theta'(0)$ (PST) and local Sherwood number $-\varphi'(0)$ are analyzed from Table 3. It depicts that by increasing k_0 and M^2, the skin friction coefficient decreases notably, while it increases with increase in γ. This implies the wall shear stress can be reduced by keeping γ as minimum. It is also observed that, the skin friction co-efficient is lower in the case of suction ($S > 0$) than that of blowing ($S < 0$). In addition, the Nusselt number qualitatively decreased with increasing in M^2, k_0, γ, A^* and B^*. But this trend is opposite for an increase in Pr. Physically speaking, when Pr is large, it means that the heat diffusion is low; as a result the thickness of the thermal boundary layer is lower. Consequently, the Nusselt number increases for higher values of Prandtl number. As expected, the Sherwood number is an increasing function of Sc, because the mass transfer analog of the Prandtl number is the Schmidt number. Further, the Sherwood number is a decreasing

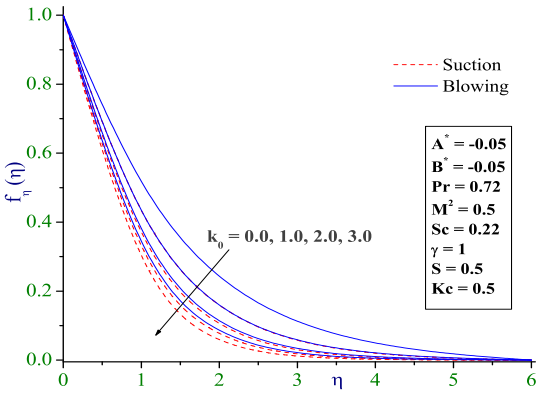

Figure 8: Effect of k_0 on velocity profile.

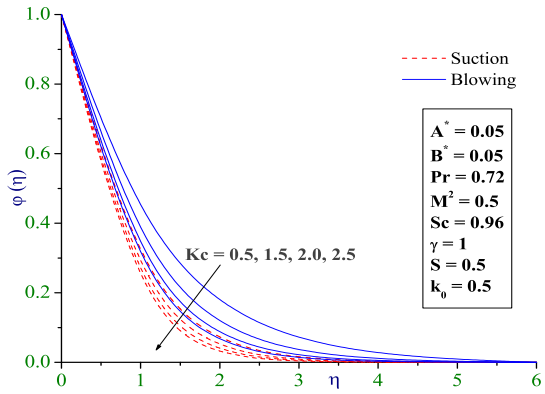

Figure 10: Effect of Kc on concentration profile.

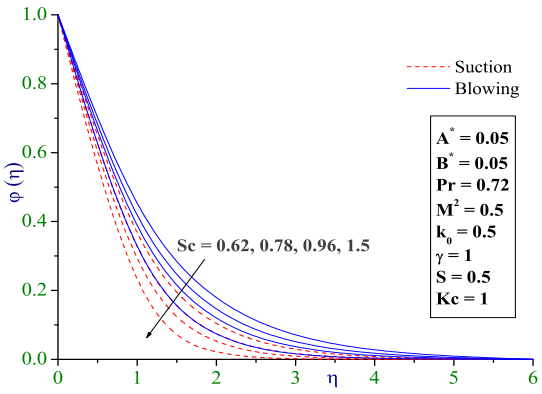

Figure 9: Effect of Sc on concentration profile.

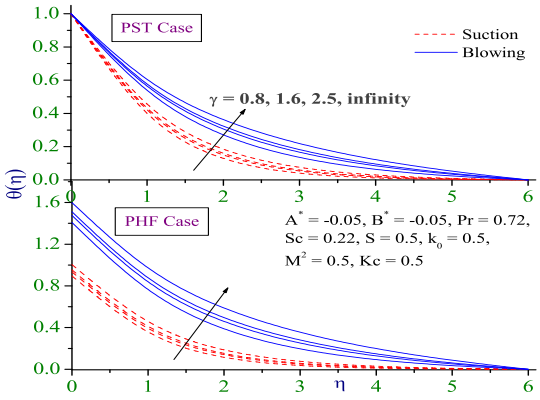

Figure 11: Effect of γ on temperature profile.

function of M^2, k_0 and γ.

Figures 2 and 3 are, respectively, plotted to depict the variation of velocity and concentration profiles against η for different values of Casson fluid parameter. Figure 2 depicts that, the horizontal velocity profile as well as momentum boundary layer thickness decreases with an increase in the Casson fluid parameter. On the other hand, the effect of increasing values of the Casson fluid parameter is responsible for solutal boundary layer thickening, which is depicted in figure 3. This result is consistent with the findings reported by Hayat et al [16]. Figures 4 and 5 represent the variation of typical velocity and concentration profiles for different values of magnetic parameter respectively. From plot 4, it is evident that, for increasing values of magnetic parameter results in flattening of horizontal velocity profiles. The transverse contraction of momentum boundary layer is due to the applied magnetic field which results in the Lorentz force producing considerable opposition to the motion. That is why; the velocity is a decreasing function of magnetic parameter. It is evident from the figure 5 that, an increase in magnetic parameter leads to increase in the concentration profile and its associated boundary layer thickness.

The Influence of blowing ($S < 0$) and suction ($S > 0$) on typical velocity profile is shown in figure 6. As expected the opposite results are found for suction and blowing effects. That is the blowing effect enhances the fluid velocity, whereas suction effect reduces the fluid velocity near the boundary. Physically, when stronger blowing is provided, then the fluid is pushed far away from the wall. As a result the viscosity of fluid decreases rapidly. Consequently, the fluid velocity is accelerated. This effect acts to increase maximum velocity within in the boundary layer. The same principle operates, but in the opposite direction in case of suction. The effect of S on the flow was the similar result observed by Eladahab

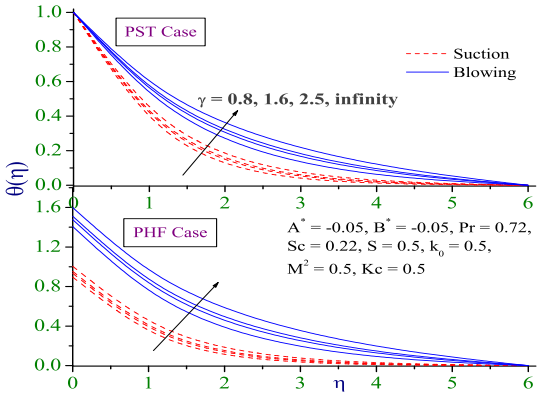

Figure 12: Effect of M^2 on temperature profile.

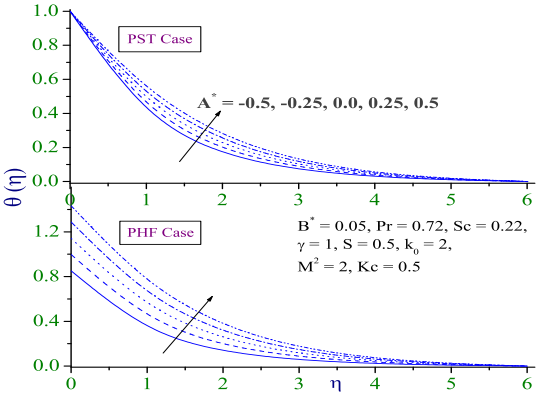

Figure 14: Effect of A^* on temperature profile.

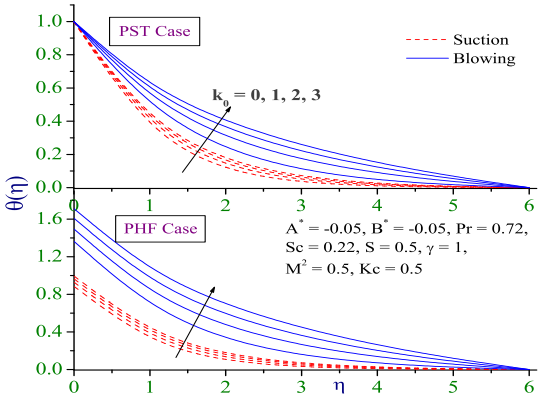

Figure 13: Effect of k_0 on temperature profile.

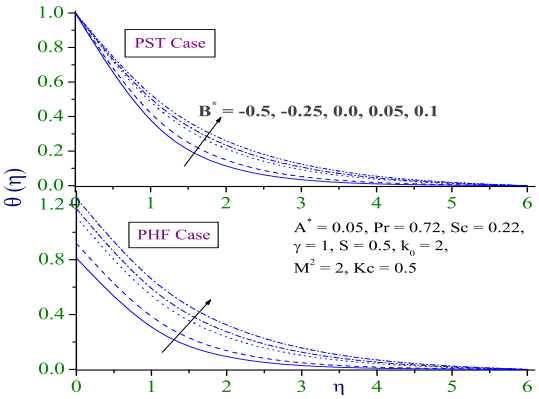

Figure 15: Effect of B^* on temperature profile.

and Aziz [33]. Figure 7 represents the variation of the typical concentration profile with respect to suction/injection parameter when other parameters are fixed. It is observed that, when suction increases the concentration profile increases and this phenomenon is quite opposite for the effect of increasing values of blowing. Further, it is observed that, the solute boundary layer for suction is thicker than that of blowing.

Figure 8 illustrates the variation of velocity distributions for different values of porous parameter. It is quite clear that the velocity profile decreased with an increase in porous parameter. This is because, the larger values of porous parameter correspond to densely pack porous medium and hence the flow rate will be reduced. The effect of porous parameter on the velocity was the similar result observed by Sheikholeslami and Ganji [25] for nanofluid. Figure 9 displays concentration profiles versus η for various values of Sc. It is elucidating that, the concentration profile decreases with an increase in Schmidt number. Because, an increase in Sc indicates the lower molecular diffusivity which results reduction in concentration profile. Hence, the concentration of species is higher for smaller value of Sc and vice versa. The chemical reaction parameter also affects the concentration distribution significantly, which can be seen from graph 10. The solute profiles and its corresponding boundary layer decreased with increasing chemical reaction parameter. The central reason for this effect is that, an increase in the chemical reaction parameter leads to increase in the number of solute molecules undergoing chemical reaction which decreases the solute field.

Figure 11 depicts the effect of Casson fluid parameter on heat transfer profile in PST and PHF cases. It is evident from this plot that, increasing values of γ results in increase in thermal boundary layer. The effect of transverse magnetic field on heat transfer profile is depicted in figure 12 for

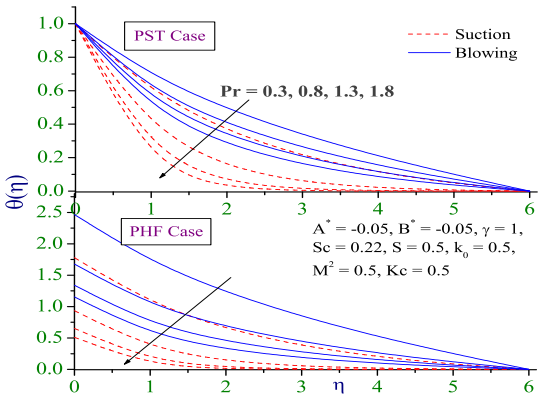

Figure 16: Effect of Pr on temperature profile.

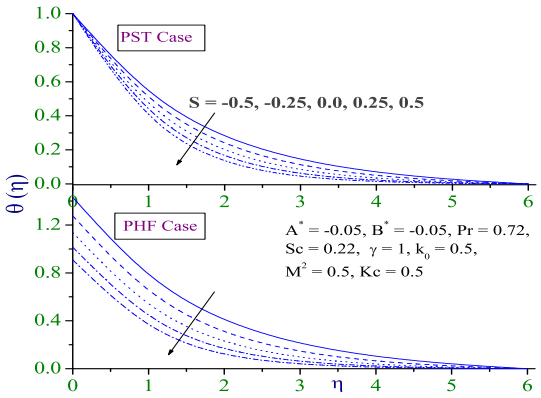

Figure 17: Effect of Sc on temperature profile.

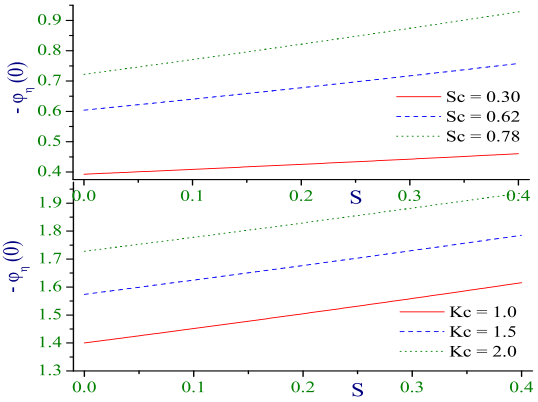

Figure 18: Effect of A^* and B^* on Nusselt number.

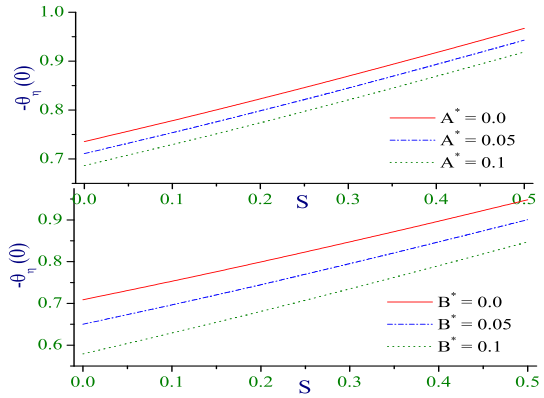

Figure 19: Effect of Sc and Kc on Sherwood number.

both PST and PHF cases. From this plot, it is observed that the transverse magnetic field contributes to the thickening of the thermal boundary layer. The resistance due to Lorentz force on the flow is responsible for enhancing the temperature profile as well as thermal boundary layer thickness. Figure 13 presents the typical temperature distribution in PST and PHF cases for various values of porous parameter. It can be seen that, the temperature profile and thermal boundary layer thickness increases with an increase in the porous parameter.

Figures 14 and 15, are respectively, illustrate the effects of both space-dependent and temperature-dependent heat source/sink parameter on temperature distributions in PST and PHF cases. Ahead of discussing the results, we recollect the fact that $A^* < 0, B^* < 0$ corresponds to heat sink and $A^* > 0, B^* > 0$ corresponds to an internal heat source. It is the cumulative influence of the space-dependent and temperature-dependent heat source/sink parameter that determines the extent to which the temperature falls or rises in the boundary layer region. From these plots it is clear that the energy is released for increasing values of $A^* > 0$ and $B^* > 0$ and this causes to an increase in the temperature field in both cases. Whereas the energy is absorbed for increasing values of $A^* < 0$ and $B^* < 0$, as a result the temperature and its corresponding boundary layer decreased. Further, the thermal boundary layer is thicker for a heat source case as compared with heat sink.

Figure 16 shows the effect of Prandtl number on temperature distribution in PST and PHF cases. It shows that, the temperature profile decreases as the Prandtl number strengthens. This is due to the fact that a higher Prandtl number fluid has relatively low thermal conductivity, which reduces the conduction as a result temper-

ature decreases. This shows that the rate of cooling is faster in case of higher Prandtl number. The variation of temperature profiles in PST and PHF cases, for various values of suction parameter is presented in figure 17. It is seen that, the temperature profile decreases in the case of blowing and increases for suction.

Finally, plot 18 depicts the effect of space-dependent heat source A^* and temperature dependent heat source parameter B^* on the Nusselt number profiles versus suction parameter. As expected the Nusselt number decreases for increasing values of space-dependent heat source A^* and temperature-dependent heat source parameter B^*. It is also observed that, the Nusselt number is lower in the absence of space and temperature dependent heat source parameter, i.e., A^* and $B^* = 0$ than in the presence. This implies that the space and temperature dependent heat source effect enhances the rate of heat transfer. The influence of Sc and Kc on the Sherwood number is plotted in figure 19. From this plot, it is observed that, The Sherwood number increases for increasing values of Sc and Kc. Interestingly, from the graphs 11-17, it is possible to see that; the thermal boundary layer for PHF case is thicker than that of PST case.

6 Conclusions

The heat and mass transfer with non-uniform heat source/sink and suction/blowing effects for a steady hydrodynamic boundary layer flow of a non-Newtonian Casson fluid past a porous stretching sheet has been studied numerically. In this study, emphasis is given on how different flow fields changes due to the variation of magnetic field, non-uniform heat source/sink, chemical reaction and suction/blowing. Some of the major findings of our analysis are listed below.

- The thickness momentum boundary layer reduces for the effect of the Casson fluid parameter, magnetic parameter and porous parameter.
- Blowing causes an increase in fluid velocity profile, whereas opposite effect is seen in the case of suction.
- Space and temperature-dependent heat sinks are desirable for effective cooling of the stretching sheet.
- Thermal boundary layer is thinner for the effect of blowing than that of suction effect.
- The effect of Prandtl number is to decrease the thermal boundary layer thickness and this manner is opposite for the effect of magnetic parameter, porous parameter and Casson fluid parameter.
- For efficient cooling of the stretching sheet, the prescribed heat flux boundary condition is better suited.
- The solutal boundary layer thickness increases for the effect of Casson fluid parameter, permeable parameter, magnetic parameter and suction parameter. This phenomena is opposite for the effect of blowing, chemical reaction parameter and Schmidt number.
- Velocity, temperature and concentration profiles much more suppresses in the case of blowing than suction.
- If $S = k_0 = 0$ and $M^2 = 0.5$, then our results coincide with the results of Hayat et al [16] for limiting cases.

Acknowledgements

The authors are very thankful to the editor and the reviewers for their constructive comments and suggestions to improve the presentation of this paper. Further, one of the authors, B.J.Gireesha expresses gratitude to University Grant Commission, New Delhi, India for financial support under RAMAN Fellowship for post doctoral research in USA.

References

[1] B. C. Sakiadis, *Boundary layer behaviour on continuous solid surface* , A. I. Ch. E. J. 7 (1961) 26-28.

[2] F. K. Tsou, E. M. Sparrow, R. J. Goldstein, *Flow and heat transfer in the boundary layer on a continuous moving surface*, Int. J. Heat Mass Transfer 10 (1967) 219-235.

[3] L. J. Crane, *Flow past a stretching sheet*, Z. Angew. Math. Phys. 21 (1970) 645-647.

[4] R. Cortell, *A note on magnetohydrodynamic flow of a power-law fluid over a stretching sheet*, Appl. Math. Comput. 168 (2005) 557-566.

[5] B. C. P. Kumara, G. K. Ramesh, A. J. Chamka, B. J. Gireesha, *Stagnation-point flow of a viscous fluid towards a stretching surface with variable thickness and thermal radiation*, Int. J. Industrial Mathematics 7 (2015) 77-85.

[6] M. Sheikholeslami, D. D. Ganji, M. M. Rashidi, *Ferrofluid flow and heat transfer in a semi annulus enclosure in the presence of magnetic source considering thermal radiation*, Journal of the Taiwan Institute of Chemical Engineers 47 (2015) 6-17.

[7] M. S. Kandelousi, *Effect of spatially variable magnetic field on ferrofluid flow and heat transfer considering constant heat flux boundary condition*, European Physical Journal Plus 129 (2014) 248.

[8] H. R. Ashorynejad, M.Sheikholeslami, I. Pop, D. D. Ganji, *Nanofluid flow and heat transfer due to a stretching cylinder in the presence of magnetic field*, Heat Mass Transfer 49 (2013) 427-436.

[9] A. Ishak, K. Jafar, N. Nazar, I. Pop, *MHD stagnation point flow towards a stretching sheet*, Phys A 388 (2009) 3377-3383.

[10] B. J. Gireesha, B. Mahanthesh, *Perturbation solution for radiating viscoelastic fluid flow and heat transfer with convective boundary condition in non-uniform channel with Hall current and chemical reaction*, ISRN Thermodynamics, 2013 (2013), Article ID 935481, 14 pages, DOI: http://dx.doi.org/10.1155/2013/935481.

[11] W. R. Schowalter, *Mechanics of non-Newtonian Fluids*, Pergamon Press, USA (1978).

[12] S. Nadeem, R.Ul Haq, N. S. Akbar, Z. H. Khan, *MHD three-dimensional Casson fluid flow past a porous linearly stretching sheet*, Alexandria Engineering Journal 52 (2013) 577-582.

[13] M. Mustafa, T. Hayat, I. Pop, A. Aziz, *Unsteady boundary layer flow of a Casson fluid due to an impulsively started moving flat plate*, Heat Transfer 40 (2011) 563-576.

[14] N. T. M. Elbade, M. G. E. Salwa, *Heat transfer of MHD non-Newtonian Casson fluid flow between two rotating cylinder*, J. Phy, Soc. Jpn. 64 (1995) 41-64.

[15] J. Boyd, J. M. Buick, S. Green, *Analysis of the Casson and Carreau-Yasuda non-Newtonian blood models in steady and oscillatory flow using the lattice Boltzmann method*, Phys. Fluids 19 (2007) 93-103.

[16] T. Hayat, S. A. Shehzad, A. Alsaedi, *Soret and Dufour effects on magetohydrodynamic (MHD) flow of Casson fluid*, Appl. Math. Mech. 33 (2012) 1301-1312.

[17] M. Mustafa, T. Hayat, I. Pop, A. Aziz, *Unsteady boundary layer flow of a Casson fluid due to an impulsive started moving flat plate*, Heat Transfers-Asian Resc. 40 (2011) 563-576.

[18] S. Nadeem, R. Ul Haq, C. Lee, *MHD flow of a Casson fluid over an exponential shrinking sheet*, Scientia Iranica 19 (2012) 1550-1553.

[19] S. Mukhopadhyay, P. Ranjan De, K. Bhattacharyya, G. C. Layek, *Casson fluid flow over an unsteady stretching surface*, Ain Shams Engineering Journal 4 (2013) 933-938.

[20] V. M. Starov, V. G. Zhdanov, *Effective viscosity and permeability of porous media*, Colloids Surf. A 192 (2001) 363-375.

[21] S. Kiwan, M. E. Ali, *Near-slit effects on the flow and heat transfer from a stretching plate in a porous medium*, Numer. Heat Transfer A 54 (2008) 93-108.

[22] M. M. Rashidi, E. Erfani, *A new analytical study of MHD stagnation-point flow in porous media with heat transfer*, Computers and Fluids 40 (2011) 172-178.

[23] A. Tamayol, K. Hooman, M. Bahrami, *Thermal analysis of flow in a porous medium over a permeable stretching wall*, Transport Porous Med. 8 (2010) 661-676.

[24] B. J. Gireesha, B. Mahanthesh, R. S. R. Gorla, *Suspended particle effect on nanofluid boundary layer flow past a stretching surface*, Journal of nanofluids 3 (2014) 267-277.

[25] M. Sheikholeslami, D. D. Ganji, *Heated permeable stretching surface in a porous medium using nanofluids*, Journal of Applied Fluid Mechanics 7 (2014) 535-542.

[26] M. M. Rashidi, D. D. Ganji, S. M. Sadri, *New analytical solution of stagnation point flow in a porous medium*, Journal of Porous Media 14 (2011) 1125-1135.

[27] M. Sheikholeslami, *Effect of uniform suction on nanofluid flow and heat transfer over a cylinder*, J. Braz. Soc. Mech. Sci. Eng. (2014) http://dx.doi.org/10.1007/s40430-014-0242-z.

[28] M. N. Tufail, A. S. Butt, A. Ali, *Heat source/sink effects on non-Newtonian MHD fluid flow and heat transfer over a permeable stretching surface: Lie group analysis*, Indian. J. Phys. 88 (2013) 75-82.

[29] S. Pramanik, *Casson fluid flow and heat transfer past an exponential porous stretching surface in presence of thermal radiation*, Ain Shams Engineering Journal 5 (2014) 205-212.

[30] A. B. Parsa, M. M. Rashidi, T. Hayat, *MHD boundary-layer flow over a stretching surface with internal heat generation or absorption*, Heat Transfer-Asian Research 42 (2013) 500-514.

[31] G. K. Ramesh, A. J. Chamkha, B. J. Gireesha, *MHD mixed convection flow of a viscoelastic fluid over an inclined surface with a non-uniform heat source/sink*, Canadian Journal of Physics 91 (2013) 1074-1080.

[32] S. Manjunatha, B. J. Gireesha, K. M. Eshwarappa, C. S. Bagewadi, *Similarity solutions for boundary layer flow of a dusty fluid through a porous medium over a stretching surface with internal heat generation/absorption*, Journal of Porous media 16 (2013) 501-514.

[33] E. M. A. Eladahab, M. A. E. Aziz, *Blowing/suction effect on hydromagnetic heat transfer by mixed convection from an inclined continuously stretching surface with internal heat generation/absorption*, Int. J. Therm, Sci. 43 (2004) 704-719.

[34] M. S. Abel, N. Mahesha, *Heat transfer in MHD viscoelastic fluid flow over a stretching with variable thermal conductivity, non-uniform heat source and radiation*, App. Math. Mod. 32 (2008) 1965-1983.

[35] D. Pal, *Hall current and MHD effects on heat transfer over an unsteady stretching permeable surface with thermal radiation*, Comp. Math. Appl. 66 (2013) 1161-1180.

[36] B. J. Gireesha, G. K. Ramesh, M. S. Abel, C. S. Bagewadi, *Boundary layer flow and heat transfer of a dusty fluid over a stretching sheet with non-uniform heat source/sink*, Int. J. of Multiphase Flow 37 (2011) 977-982.

Bijjanal Jayanna Gireesha is a Assistant Professor in Department of Mathematics at Kuvempu University, Karnataka and received M.Phil (1999) and Ph.D (2002) in Fluid Mechanics from Kuvempu University, Shimoga, India. Currently he is working as a visiting research faculty in Department of Mechanical Engineering Cleveland State University, Cleveland, USA. His research interests include the areas of Fluid mechanics particularly, boundary layer flows, Newtonian/ non-Newtonian fluids, heat and mass transfer, Nanofluid flow problems

Basavarajappa Mahanthesh is born in Davangere, Karnataka, INDIA in 1989. He received his M.Sc. in Kuvempu University, Shimoga, India. He joined as a Research Scholar in the Department of Mathematics, Kuvempu University in 2013 and he is continuing research till now. His research interests are three-dimensional boundary layer flows, fluid-particle suspension, nanofluids and Heat/Mass transfer.

Mohammad Mehdi Rashidi is born in Hamedan, Iran in 1972. He received his B.Sc. degree in Bu-Ali Sina University, Hamedan, Iran in 1995. He also received his M.Sc. and Ph.D degrees from Tarbiat Modares University, Tehran, Iran in 1997 and 2002, respectively. His research focuses on Heat and Mass Transfer, Wind Tunnel, Thermodynamics, Computational Fluid Dynamics (CFD), Nonlinear Analysis, Engineering Mathematics, Exergy and Second Law Analysis, Numerical and Experimental Investigations of Nanofluids Flow for Increasing Heat Transfer and Study of Magnetohydrodynamic Viscous Flow. He is a professor of Mechanical Engineering at Tongji University, Shanghai, China. He has published two books: Advanced Engineering Mathematics with Applied Examples of MATHEMATICA Software (2007) (320 pages) (in Persian), and Mathematical Modelling of Nonlinear Flows of Micropolar Fluids (Germany, Lambert Academic Press, 2011). His works have been published in the Plos One, Energy, Computers and Fluids, Communications in Nonlinear Science and Numerical Simulation and several other peer-reviewed international journals. He has published over 180 (110 of them are indexed in Scopus) journal articles and 45 conference papers.